IL-22 produced by ILC3 mediates epithelial fucosylation

We next investigated how ILC3 induce epithelial fucosylation. ILC3 cells secrete IL-22, which stimulates the antimicrobial function and maintenance of intestinal ECs (*3*, *4*, *36*, *38*). Indeed, the expression of *Il22* gene was much higher in ILC3 than in any other intestinal immune cell subset (fig. S7A). We therefore assessed whether commensal bacteria regulate ILC3 differentiation and cytokine expression. Although AB-treated or wild-type mice had similar numbers of CD3$^-$ RORγt$^+$

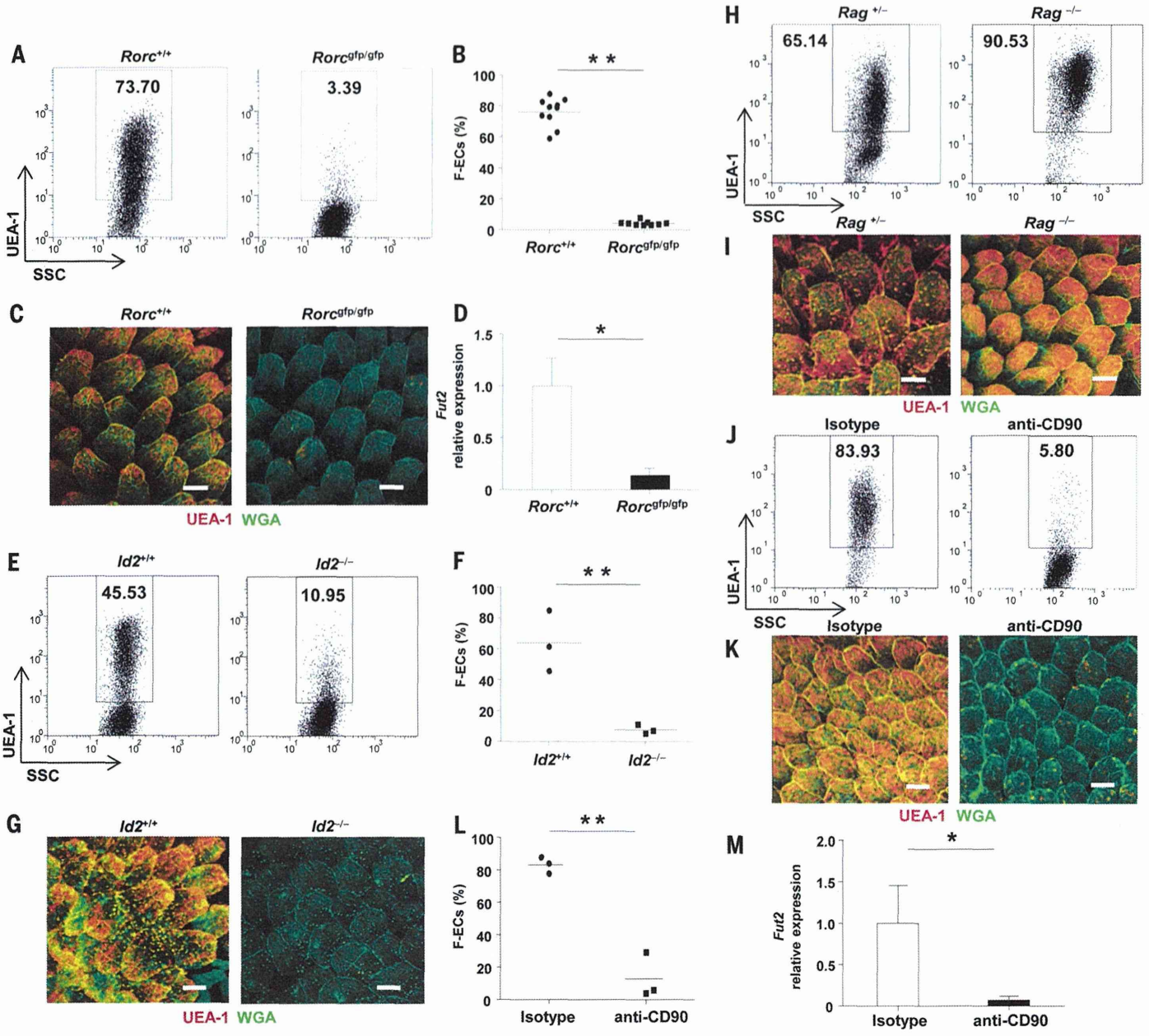

Fig. 3. CD90$^+$ RORγt$^+$ ILC3 induce F-ECs. (**A** and **B**) Representative dot-plots (A) and percentages and means (B) (horizontal bars) of ileal F-ECs isolated from *Rorc*$^{+/+}$ and *Rorc*$^{gfp/gfp}$ mice (n = 10 mice per group). SSC, side scatter. $^{**}P < 0.01$ by using Student's t test. Data of two independent experiments are combined. (**C**) Whole-mount ileal tissues from *Rorc*$^{+/+}$ and *Rorc*$^{gfp/gfp}$ mice were stained with UEA-1 (red) and WGA (green) (n = 10 mice per group). Scale bars, 100 μm. Data are representative of two independent experiments. (**D**) Expression of *Fut2* in ileal ECs isolated from *Rorc*$^{+/+}$ and *Rorc*$^{gfp/gfp}$ mice (n = 5 mice per group). Data are representative of two independent experiments. Error bars indicate SD. $^{*}P < 0.05$. (**E** and **F**) Representative dot-plots (E) and percentages and means (F) (horizontal bars) of ileal ECs isolated from *Id2*$^{+/+}$ and *Id2*$^{-/-}$ mice (n = 3 mice per group). Data of three independent experiments are combined. (**G**) Whole-mount staining of ileal villi isolated from *Id2*$^{+/+}$ and *Id2*$^{-/-}$ mice. Scale bars, 100 μm. Data are representative of three independent experiments. (**H** and **J**) Representative dot-plots of ileal ECs isolated from *Rag*$^{+/-}$ and *Rag*$^{-/-}$ mice (H) and *Rag*$^{-/-}$ mice treated with mAb to CD90 (anti-CD90 mAb) or isotype control Ab to CD90 (J) (n = 3 mice per group). (**I** and **K**) Whole-mount staining of ileal villi isolated from *Rag*$^{+/-}$ or *Rag*$^{-/-}$ mice (I) and anti-CD90 mAb– or anti-CD90 isotype control Ab–treated *Rag*$^{-/-}$ mice (K) (n = 3 mice per group). Scale bars, 100 μm. Data are representative of two independent experiments. (**L** and **M**) Percentages and means (horizontal bars) of ileal F-ECs (L) and *Fut2* expression (M) isolated from anti-CD90 mAb– or isotype control Ab–treated *Rag*$^{-/-}$ mice (n = 3 mice per group). Data are representative of two independent experiments. Error bars indicate SD. $^{*}P < 0.05$, $^{**}P < 0.01$ by using Student's t test.

ILC3 (fig. S7, B and C), expression of IL-22 was significantly reduced in AB-treated mice but was restored after cessation of AB treatment (fig. S7D). To identify whether IL-22 is involved in the induction of F-ECs, we analyzed mice lacking IL-22 and found that they had reduced numbers of F-ECs; this was correlated with a decrease in epithelial *Fut2* expression (Fig. 4, A and B). We next examined whether IL-22 alone induced epithelial fucosylation. We used hydrodynamic delivery of an *Il22*-encoding plasmid vector so as to ectopically overexpress IL-22 in AB-treated mice (fig. S8, A and B). In both AB-treated wild-type and $Rorc^{gfp/gfp}$ mice, F-ECs were induced in both the duodenum (part 1) and the ileum (part 4) in mice ectopically producing IL-22 but not in mice receiving control vector (Fig. 4, C and D, and fig. S8, C and D). This suggests that IL-22 is sufficient for epithelial fucosylation. Expression of *Fut2* was correlated with the presence of IL-22–induced F-ECs (Fig. 4E). To confirm whether IL-22 produced by ILC3 is necessary for epithelial fucosylation, Rag-deficient mice were treated with an antibody in order to neutralize IL-22. Epithelial *Fut2* expression and fucosylation were interrupted by the neutralization of IL-22 (Fig. 4, F to H). Microbial analyses of IL-22–deficient and

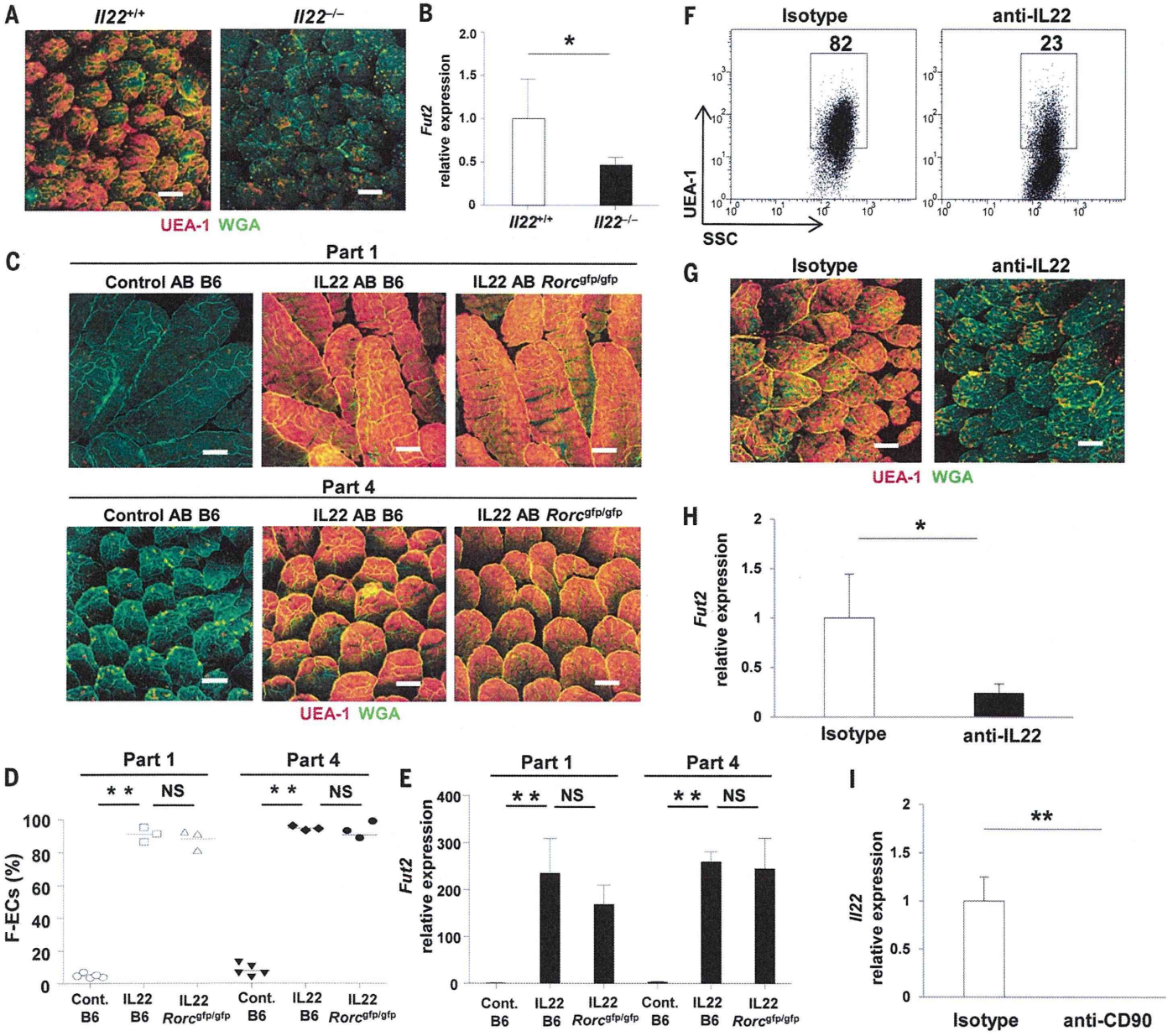

Fig. 4. IL-22 produced by ILCs is involved in the induction of F-ECs. (**A** and **B**) Whole-mount tissues stained with UEA-1 (red) and WGA (green) (A) and gene expression of *Fut2* (B) in ileal villi isolated from $Il22^{+/+}$ or $Il22^{-/-}$ mice (n = 6 mice per group). Error bars indicate SD. *P < 0.05 by using Student's t test. Scale bars, 100 μm. Data are representative of two independent experiments. (**C** to **E**) AB-treated C57BL/6 (B6) or $Rorc^{gfp/gfp}$ mice were intravenously injected with IL-22–encoding plasmid or control vector. Whole-mount staining (C), frequency of F-ECs (D) (mean, horizontal bars), and Fut2 mRNA expression was analyzed by means of rRT-PCR ($n \geq 3$ mice per group) (E). Scale bars, 100 μm. Error bars indicate SD. **P < 0.01 by using Student's t test. NS, not significant. Data are representative of two independent experiments. (**F** to **H**) Representative dot-plots (F), whole-mount histological images (G), and expression of *Fut2* (H) of ileal ECs isolated from $Rag^{-/-}$ mice treated with antibody to IL-22 or control Ab. Scale bars, 100 μm. Error bars indicate SD. *P < 0.05 by using Student's t test. (**I**) Expression of *Il22* in ileal LP cells from $Rag^{-/-}$ mice treated with antibody to CD90 or control Ab. Error bars inidicate SD. **P < 0.01 by using Student's t test. Data are representative of two independent experiments.

antibody-to-IL-22–treated Rag-deficient mice revealed the presence of SFB (fig. S6, A and B). These findings demonstrate that ILC3-derived IL-22 induced by commensal bacteria mediates epithelial fucosylation. Furthermore, depletion of ILC3 by injecting antibody to CD90 into Rag-deficient mice resulted in marked reduction of IL-22 expression (Fig. 4I), supporting the notion that IL-22–mediated signals produced by ILC3 are a key part of the EC fucosylation cascade. IL-22R is composed of two subunits, IL-22R1 and IL-10Rβ (*39*). Whereas IL-10Rβ was ubiquitously expressed, expression of IL-22R1 was specifically detected in intestinal ECs and was not reduced, even after the depletion of commensal bacteria (fig. S9, A and B). Taken together, our findings indicate that commensal bacteria provide signals that prompt ILC3 to produce IL-22, which leads to the induction of Fut2 by IL-22R–positive intestinal ECs.

LTα expressed by ILC3 induces epithelial fucosylation

ILC3 support the development and maintenance of secondary lymphoid tissues through the expression of lymphotoxins (LTs)—especially LTα1β2 (*40*). The expression of *Lta* and *Ltb* genes was higher in ILC3 than in any other intestinal immune cell subset (fig. S10A). In contrast to IL-22, which was induced by commensal bacteria, *Lta* and *Ltb* gene expression in ILC3 was not affected by commensal flora because the AB treatment did not alter the gene expression (fig. S10B). However, intestinal epithelial fucosylation and *Fut2* expression were severely impaired in $Lta^{-/-}$ mice (Fig. 5, A to C). $Lta^{-/-}$ mice possess congenital defects in secondary lymphoid organs (*41*). To elucidate the contribution of LTα to epithelial fucosylation in adult mice that have established secondary lymphoid organs, wild-type mice were treated with LTβR-Ig, which blocks LTα1β2 signaling. Epithelial fucosylation was attenuated by treatment with LTβR-Ig (Fig. 5, D to E), implying that a continuous LT signal is required for epithelial fucosylation. To investigate whether LTα in *ILC3* is crucial for the induction of F-ECs, we constructed mixed bone marrow (BM) chimeric mice by transferring BM cells taken from

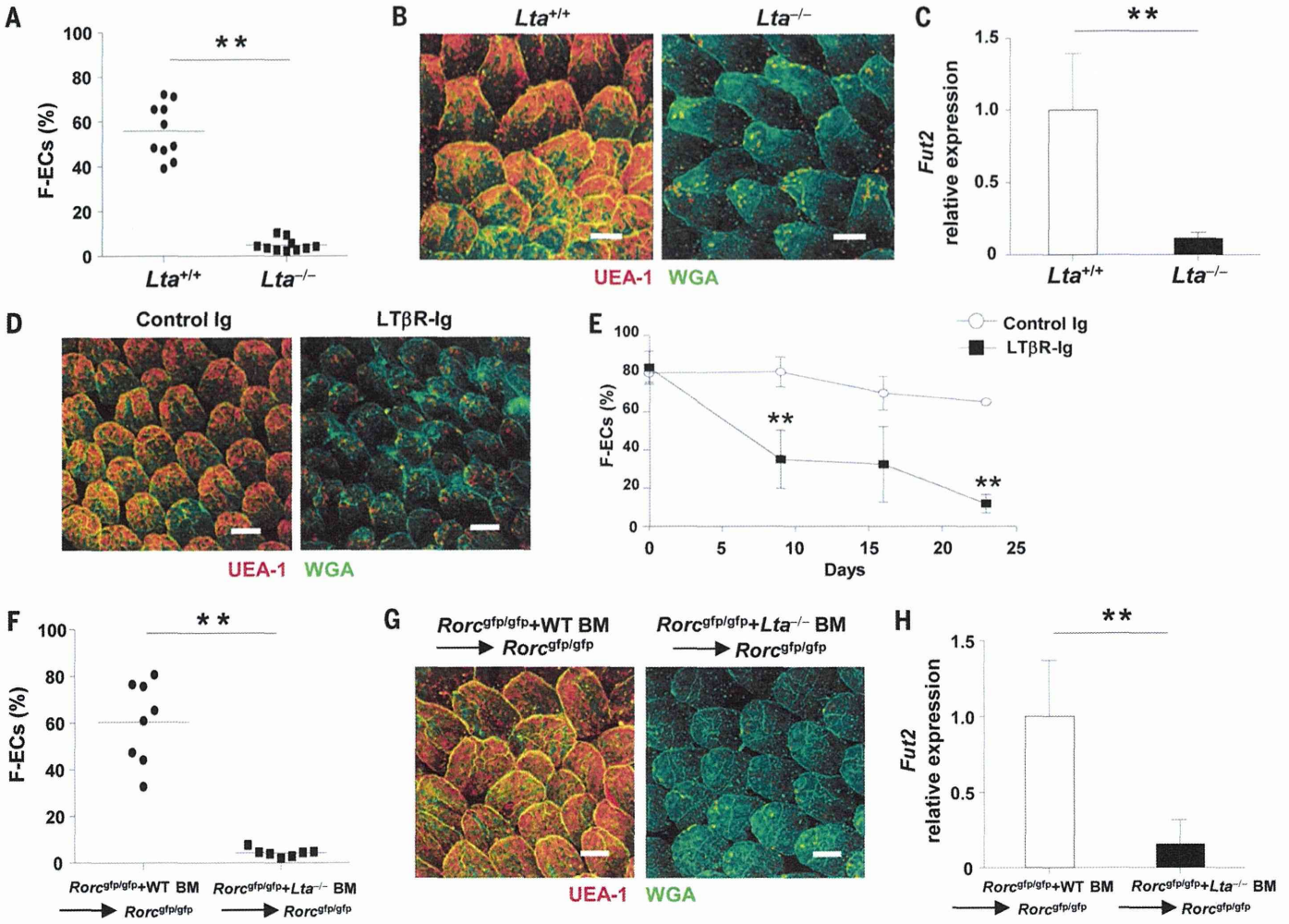

Fig. 5. LTs in innate lymphoid cells induce F-ECs. (**A**) Representative values and means (horizontal bars) of frequency of ileal F-ECs isolated from $Lta^{+/+}$ or $Lta^{-/-}$ mice (n = 10 mice per group). Data of two independent experiments are combined. $^{**}P < 0.01$ by using Student's t test. (**B**) Representative whole-mount staining of ileal villi isolated from $Lta^{+/+}$ or $Lta^{-/-}$ mice (n = 10 mice per group). Scale bars, 100 μm. (**C**) Expression of *Fut2* in ileal ECs isolated from $Lta^{+/+}$ or $Lta^{-/-}$ mice (n = 5 mice per group). Error bars inidicate SD. $^{**}P < 0.01$ by using Student's t test. Data are representative of two independent experiments. (**D**) Representative whole-mount staining of ileal villi from C57BL/6 mice injected with control IgG or LTβR-Ig. Tissues were stained with UEA-1 (red) and WGA (green). (n = 3 mice per group) (**E**) Frequencies of F-ECs in the ileum of C57BL/6 mice injected with control IgG (control Ab) or LTβR-Ig twice (day 9), 3 times (day 16), or 4 times (day 23) (n = 3 mice per group). Error bars indicate SD. $^{**}P < 0.01$ by using Student's t test. (**F** to **H**) Values and means (F), representative whole-mount staining (G), and expression of *Fut2* (H) in ileal ECs isolated from $Rorc^{gfp/gfp}$ mice injected with a mixture of BM cells from $Rorc^{gfp/gfp}$ and WT mice or $Rorc^{gfp/gfp}$ and $Lta^{-/-}$ mice (n = 7 to 8 mice per group). Data of two independent experiments are combined. Error bars indicate SD. $^{**}P < 0.01$ by using Student's t test. Scale bars, 100 μm.

LTα-deficient or -sufficient mice and mixed with BM cells from RORγt-deficient mice into lethally irradiated recipients. F-ECs and *Fut2* expression were diminished in recipient mice reconstituted with BM cells containing LTα-deficient RORγt$^+$ ILC3, whereas substantial numbers of F-ECs, and *Fut2* expression, were induced in recipient mice reconstituted with BM cells containing LTα-sufficient RORγt$^+$ ILC3, indicating the importance of LTα expressed by ILC3 in the induction of F-ECs (Fig. 5, F to H). When the microbiota of LTα-deficient mice or of mixed BM chimeras containing LTα-deficient ILC3 were examined, substantial numbers of SFB were observed (fig. S6, A and B). From these results, we concluded that induction and maintenance of F-ECs were also regulated by ILC3-derived LT in a commensal flora–independent manner.

Epithelial fucosylation protects against infection by *Salmonella typhimurium*

We next investigated the physiological role of epithelial fucosylation. With exception of Paneth cells, the *Fut2* expression and ileal epithelial fucosylation observed in wild-type mice were abolished in *Fut2*$^{-/-}$ mice (fig. S11, A to E). We did not detect any overt changes in mucosal leukocyte populations or in IL-22 or LT expression in ILC3 in these mice (fig. S11F and table S1). Epithelial fucosylation provides an environmental platform for colonization by *Bacteroides* species (*6*–*9*); however, it is unknown whether epithelial fucosylation affects colonization and subsequent infection by pathogenic bacteria. To assess the effects of intestinal fucosylation on pathogenic bacterial infection, we first infected GF mice with the enteropathogenic bacterium *Salmonella typhimurium*, which has the potential to attach to fucose-containing carbohydrate molecules (*42*). After infection with *S. typhimurium*, ECs from both part 1 (duodenum) and part 4 (ileum) of the mouse intestine were fucosylated, and this was correlated with Fut2 expression (Fig. 6, A and B). Previous reports have shown that expression of IL-22 in ILCs is much higher in mice infected with *S. typhimurium* (*43*, *44*). Therefore, *S. typhimurium*–induced epithelial fucosylation may be mediated by ILC3. Indeed, epithelial fucosylation was not induced in RORγt-deficient mice after *S. typhimurium* infection (Fig. 6C). To investigate whether epithelial fucosylation has a role in regulating pathogenic bacterial infection, we infected wild-type or *Fut2*$^{-/-}$ mice with *S. typhimurium* and examined disease progression. Compared with wild-type mice, *Fut2*$^{-/-}$ mice were more susceptible to *Salmonella* infection accompanied with the observation of severe inflamed cecum (Fig. 6D). Consistent with the inflammatory status of diseased mice, the numbers of infiltrating leukocytes in cecum were higher in *Fut2*$^{-/-}$ mice than in wild-type mice (Fig. 6E). Although *S. typhimurium* titers in cecal contents were comparable between wild-type and *Fut2*$^{-/-}$ mice, increased numbers of *S. typhimurium* infiltrated the cecal tissue of *Fut2*$^{-/-}$ mice (Fig. 6F). These results suggest that epithelial fucosylation is dispensable for luminal colonization by *S. typhimurium* but inhibits bacterial invasion of intestinal

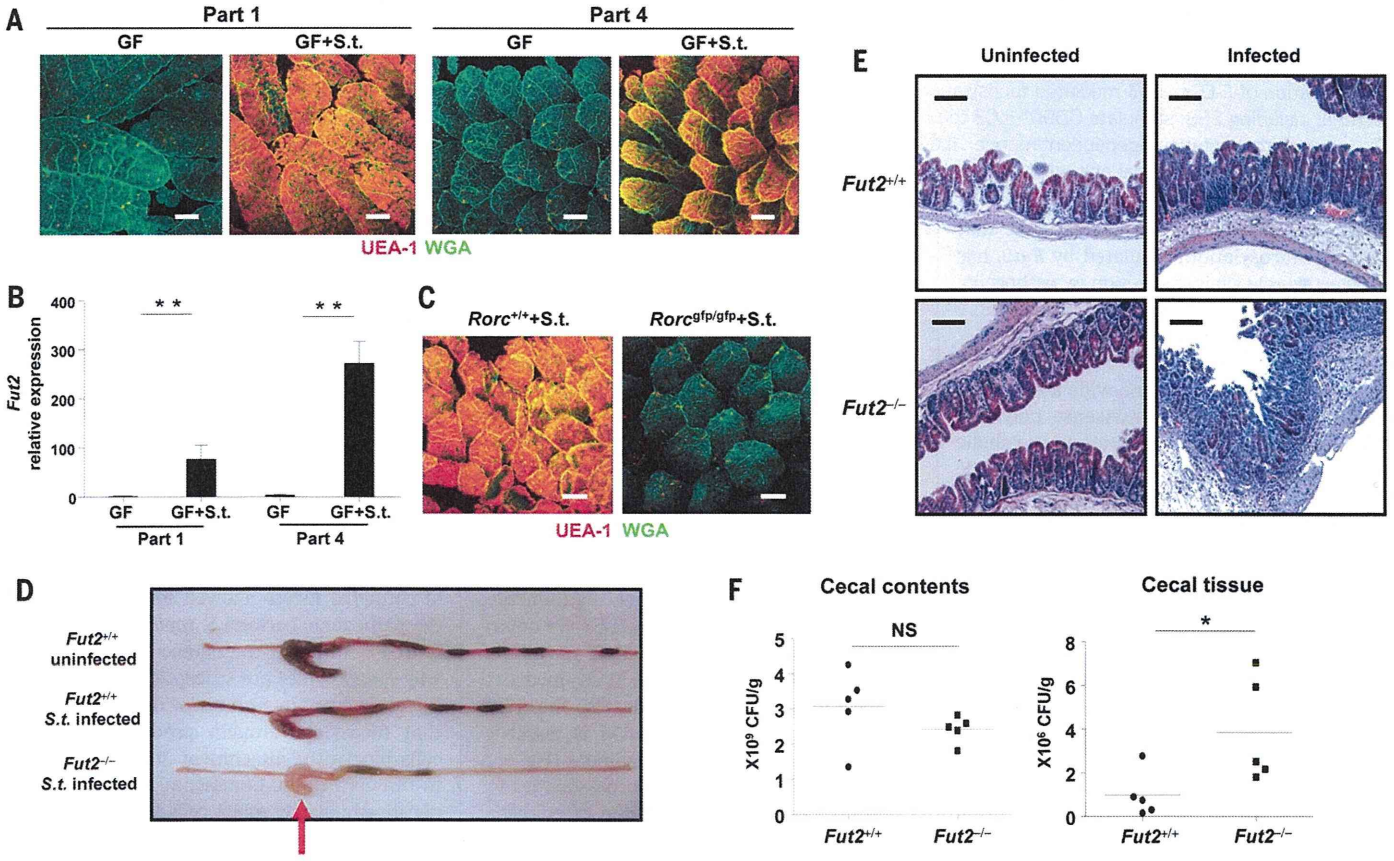

Fig. 6. Epithelial fucosylation protects against infection by *S. typhimurium*. (**A**) Whole-mount tissues from part 1 (duodenum) and part 4 (ileum) of the small intestines of germ-free (GF) or *S. typhimurium*–infected GF mice were stained with UEA-1 (red) and WGA (green) (n = 3 to 4 mice per group). Scale bars, 100 μm. (**B**) Epithelial Fut2 expression in part 1 and part 4 of the small intestines of GF and *S. typhimurium*–infected GF mice was analyzed by using quantitative PCR (n = 3 to 4 mice per group). Error bars indicate SD. $^{**}P < 0.01$ by using Student's t test. (**C**) Whole-mount tissues from ileum of *S. typhimurium*–infected *Rorc*$^{+/+}$ or *Rorc*$^{gfp/gfp}$ mice were isolated and stained with UEA-1 (red) and WGA (green) (n = 3 to 4 mice per group). Scale bars, 100 μm. (**D** and **E**) *Fut2*$^{+/+}$ or *Fut2*$^{-/-}$ mice were infected with *S. typhimurium*. Red arrow shows inflammation of the cecum. Representative macroscopic images (D) and hematoxylin and eosin–stained cecal sections (E) of infected or uninfected mice (n = 5 mice per group). Scale bars, 100 μm. (**F**) Numbers of bacteria in the luminal contents, and within the tissues, of the ceca of *Fut2*$^{+/+}$ or *Fut2*$^{-/-}$ mice were counted 24 hours after infection (n = 5 mice per group). $^{*}P < 0.05$ by using Student's t test. NS, not significant. Three independent experiments were performed with similar results.

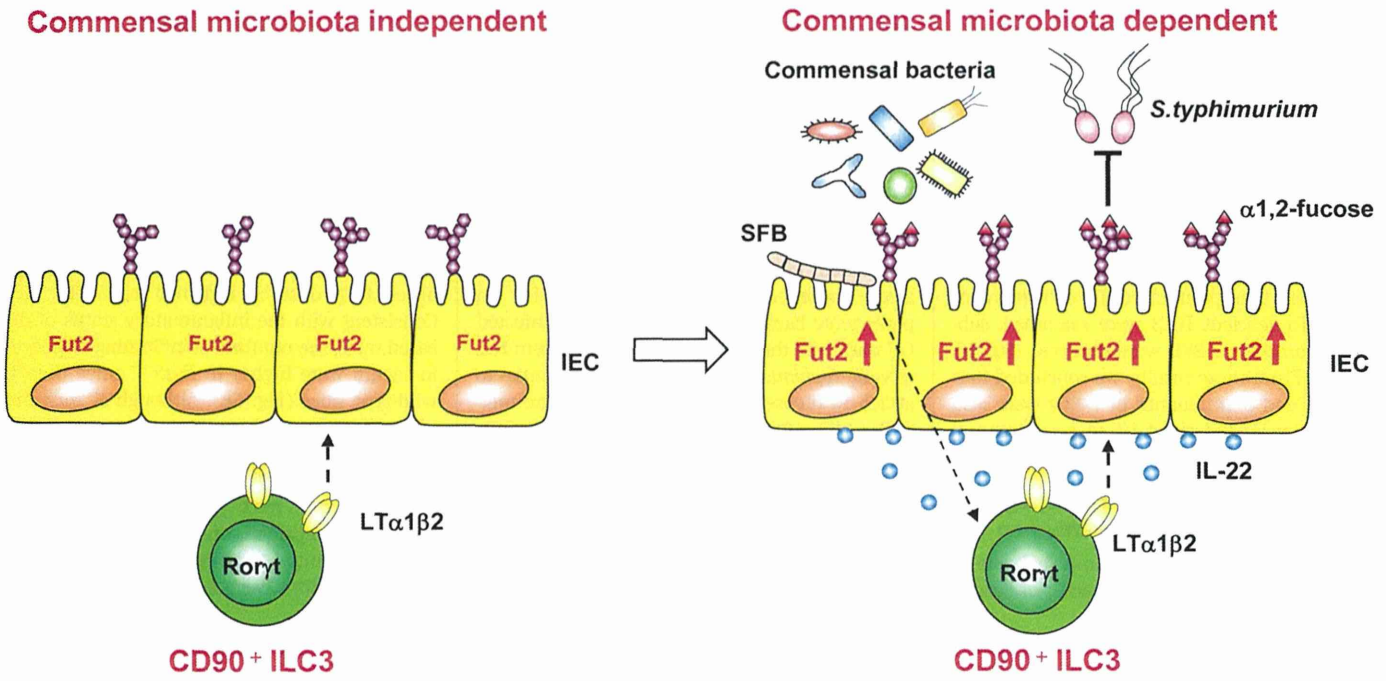

Fig. 7. Scheme for the induction and regulation of epithelial fucosylation by ILC3. IL-22– and LTα-producing ILC3 are critical cells for the induction and regulation of F-ECs. ILC3-mediated fucosylation of ECs is operated by commensal microbiota–dependent and –independent manners. Commensal bacteria, including SFB, stimulate CD90$^+$ ILC3 to produce IL-22 for the induction of Fut2 in ECs. On the other hand, LTα production by ILC3 are operated by a commensal bacteria–independent manner. ILC3-derived IL-22 and LTα induce Fut2 and subsequent epithelial fucosylation, which inhibits infection by *S. typhimurium*. IEC, intestinal epithelial cell.

tissues. Collectively, these results indicate that epithelial fucosylation, regulated by *Fut2*, has a protective role against infection by pathogenic bacteria.

Discussion

The results of recent genome-wide association studies imply that FUT2 nonsense polymorphisms affect the incidence of various metabolic and inflammatory diseases, including chronic intestinal inflammation such as Crohn's disease and infections with pathogenic microorganisms, especially Norwalk virus and rotavirus in humans (*13*–*19*). Understanding the mechanisms of regulation of Fut2 gene expression and fucosylation, one of the major glycosylation events in intestinal ECs, is therefore of great interest. Previously, it was thought that epithelial fucosylation is initiated by direct interaction between commensals and ECs (*7*). Indeed, several reports have shown that epithelial fucosylation is actively induced and used by *Bacteroides* (*8*, *9*). Here, we unexpectedly found that microbiota–epithelia cross-talk is insufficient to induce epithelial fucosylation, and rather, CD90$^+$ RORγt$^+$ ILC3 are necessary for induction of epithelial *Fut2* expression and consequent fucosylation. ILC3 located in the intestinal lamina propria express high levels of IL-22 in a commensal bacteria–dependent manner (Fig. 4I and fig. S7, A and D). This IL-22 then presumably binds to IL-22R expressed by intestinal ECs, leading to the induction of Fut2 and initiation of the EC fucosylation process (Fig. 7). In contrast to the expression of IL-22, ILC3 express LT in a commensal bacteria–independent manner. Spontaneous expression of LT on ILC3 also contributes to the induction of epithelial fucosylation. To explain the mechanism underlying induction of epithelial fucosylation, we propose that epithelial fucosylation is regulated by a two-phase system orchestrated by ILC3 through the microbiota-independent production of LT and the induction of IL-22 by commensal bacteria (Fig. 7). Although other types of stimulation may also affect epithelial fucosylation, our findings reveal a critical role for ILC3.

Our results demonstrated that IL-22 produced by ILC3 is necessary and sufficient for induction of epithelial fucosylation when ILC3 are appropriately stimulated by commensal microbiota (Fig. 4, A to E). In addition to IL-22–mediated epithelial fucosylation, our results also show that the level of epithelial fucosylation is markedly reduced under LTα-deficient conditions (Fig. 5, A to C). Our findings suggest two possibilities for the IL-22/LT-mediated regulation of epithelial fucosylation. The first is that Fut2 expression and subsequent epithelial fucosylation are induced when the intensity of synergistic or additive signals from IL-22 and LT is above the threshold for activation of Fut2. For example, LT produced by ILC3 provides the baseline signal for the minimum expression of Fut2, whereas commensal-mediated IL-22 produced by ILC3 drives the maximum expression of Fut2 for the induction of epithelial fucosylation. The second possibility is that LT directly or indirectly regulates the expression of IL-22R by ECs, and vice versa, and/or the expression of IL-22. Indeed, a previous report has shown that LT produced by ILC3 regulates the expression of IL-23 by intestinal dendritic cells, as well as the subsequent production of IL-22 by ILC3 after infection with *C. rodentium* (*45*). How ILC3-derived IL-22 and LT regulate epithelial Fut2 expression remains to be further elucidated.

Our findings provide further evidence of the critical roles of commensal microbiota, epithelial cells, and innate immune cells (such as ILC3) in the creation of a protective platform against infection by pathogenic bacteria (Fig. 7). Ablation of epithelial fucose allowed severe infection by the pathogenic bacteria *S. typhimurium* (Fig. 6, D to F). Although the detailed mechanisms of why *Fut2*$^{-/-}$ mice are susceptible to *Salmonella* infection remain unknown, one possibility is that fucosylated mucin produced by goblet cells blocks the attachment of *S. typhimurium* to the epithelium. Commensal microbes continuously stimulated goblet cells to release fucosylated mucin into the intestinal lumen (Fig. 2C). Indeed, in a previous in vitro study, H-type 2 antigens, which are synthesized by Fut2 in intestinal ECs, prevented the binding of *S. typhimurium* to fucosylated epithelia; this supports our present findings (*42*). Our findings suggest a protective role for ILC3-mediated mucus-associated fucosylated glycan against infection by pathogenic bacteria.

ILC3 play critical roles in regulation of immune responses during mucosal infection, especially

by producing IL-22, which promotes subsequent expression of the antimicrobial molecule RegIIIγ by ECs (*4*, *36*, *45*). In addition to this, our results describe a previously unknown biological role for ILC3 in the induction and maintenance of intestinal epithelial glycosylation, which leads to the creation of an antipathogenic bacterial platform in the intestine (Fig. 7). Furthermore, epithelial fucosylation contributes to the creation of a cohabitation niche for the establishment of normal commensal microbiota (*20*, *21*). Thus, ILC3-mediated control of epithelial-surface glycosylation might represent a general strategy for regulating the gut microenvironment. Targeted modification of these mechanisms has the potential to provide novel approaches for the control of intestinal infection and inflammation.

Materials and Methods

Mice

C57BL/6 and BALB/c mice were purchased from CLEA Japan (Tokyo, Japan). *Fut2*$^{-/-}$ and *Il22*$^{-/-}$ mice (C57BL/6 background) were generated as described previously, and *Id2*$^{-/-}$ mice were kindly provided by Y. Yokota (*33*, *46*, *47*). *Fut2*$^{-/-}$ mice were crossed onto the BALB/c background for six generations. *Rag2*$^{-/-}$ mice were kindly provided by F. Alt. *Rag1*$^{-/-}$; *Rorc*$^{gfp/gfp}$, *Il6*$^{-/-}$, *Ltα*$^{-/-}$, *Tcrβ*$^{-/-}δ^{-/-}$, and *Igh6*$^{-/-}$ mice were purchased from The Jackson Laboratory. Antibiotic-treated mice were fed a cocktail of broad-spectrum antibiotics—namely, ampicillin (1 g/L; Sigma, Bandai, Japan), vancomycin (500 mg/L; Shionogi, Osaka, Japan), neomycin (1 g/L; Sigma), and metronidazole (1 g/L; Sigma)—or were given these antibiotics in their drinking water, for 4 weeks as previously described (*48*). These mice were maintained in the experimental animal facility at the University of Tokyo. GF and SFB or *L. murinus* gnotobiotic mice (BALB/c) were maintained in the GF animal facility at the Yakult Central Institute and at the University of Tokyo. In all experiments, littermates were used at 6 to 10 weeks of age.

Isolation of bacterial DNA

The isolation protocol for bacterial DNA was adapted from a previously described method (*49*), with some modifications. Bacterial samples in the duodenum and ileum were obtained from mice aged 8 weeks. After removal of PPs and intestinal contents, the intestinal tissues were washed three times with phosphate-buffered saline (PBS) for 10 s each time so as to collect bacteria embedded within the intestinal mucus for analysis of microbial composition. These bacteria-containing solutions were centrifuged, and the pellets were suspended in 500 μL of TE buffer (10 mM Tris-HCl, 1 mM EDTA; pH 8.0). Glass beads, Tris-phenol buffer, and 10% sodium dodecyl sulfate (SDS) were added to the bacterial suspensions, and the mixtures were vortexed vigorously for 10 s by using a FastPrep FP100 A (BIO 101). After incubation at 65°C for 10 min, the solutions were vortexed and incubated again at 65°C for 10 min. Bacterial DNA was then precipitated in isopropanol, pelleted by centrifugation, washed in 70% ethanol, and resuspended in TE buffer. Extracted bacterial DNA was subjected to 16*S* rRNA gene clone library (*50*).

16S rRNA gene clone library analyses

For 16*S* rRNA gene clone library analyses, bacterial 16*S* rRNA gene sequences were amplified by means of polymerase chain reaction (PCR) with the 27F (5′-AGAGTTTGATCCTGGCTCAG-3′) and 1492R (5′-GGTTACCTTGTTACGACTT-3′) primers. Amplified 16*S* rDNA was ligated into the pCR4.0 TOPO vector (Invitrogen, Carlsbad, CA), and the products of these ligation reactions were then transformed into DH-5α–competent cells (TOYOBO, Osaka, Japan). Inserts were amplified and sequenced on an ABI PRISM 3100 Genetic Analyzer (Applied Biosystems, Foster City, CA). The 27F and 520R (5′-ACCGCGGCTGCTGGC-3′) primers and a BigDye Terminator cycle sequencing kit (Applied Biosystems) were used for sequencing. Bacterial sequences were identified by means of Basic Local Alignment Search Tool (BLAST) and Ribosomal Database Project searches (*50*).

Immunohistochemistry

Immunohistochemical analyses were performed as previously described, with some modifications (*51*). For whole-mount immunofluorescence staining, the mucus layer was removed by flushing the small intestine with PBS; then, the appropriate parts of the small intestine were fixed with 4% paraformaldehyde for 3 hours. After being washing with PBS, whole-mount tissues were stained for at least 3 hours at 4°C with 20 μg/mL UEA-1 conjugated to tetramethylrhodamine B isothiocyanate (UEA-1-TRITC; Vector Laboratories, Burlingame, CA) and 10 μg/mL wheat germ agglutinin (WGA) conjugated to Alexa Fluor 633 (Invitrogen). For whole-mount fluorescence in situ hybridization analysis, we modified the protocol previously described (*52*). After fixation with 4% paraformaldehyde, intestinal tissues were washed with 1 mL PBS and 100 μL hybridization buffer (0.9 M NaCl, 20 mM Tris-HCl, 0.1% SDS) containing 2 μg EUB338 probe (5′-GCTGCCTCCCGTAGGAGT-3′) conjugated to Alexa Fluor 488 (Invitrogen). After overnight incubation at 42°C, the tissues were washed with 1 mL PBS and stained for 3 hours with 10 μg/mL WGA conjugated to Alexa Fluor 633 in PBS. After being washed with PBS, all tissues were analyzed under a confocal laser-scanning microscope (TCS SP2; Leica Microsystems, Wetzlar, Germany).

Cell preparations

A standard protocol was used to prepare intestinal ECs (*53*). Tissues of the small intestine were extensively rinsed with PBS after removal of PPs. After the intestinal contents had been removed, the samples were opened longitudinally and cut into 1-cm pieces. These tissue pieces were mildly shaken in 1 mM EDTA/PBS for 10 min at 37°C. After passage through a 40-μm mesh filter, intestinal ECs were resuspended in minimum essential medium containing 20% fetal calf serum (FCS). Lamina propria (LP) cells were collected as previously described (*54*), with some modifications. Briefly, isolated small intestine was shaken for 40 min at 37°C in RPMI 1640 containing 10% FCS and 1 mM EDTA. Cell suspensions, including intestinal ECs and intraepithelial lymphocytes, were discarded, and the remaining tissues were further digested with continuous stirring for 60 min at 37°C with 2 mg/mL collagenase (Wako) in RPMI 1640 containing 10% FCS. After passage through a 190-μm mesh, the cell suspensions were subjected to Percoll (GE Healthcare) density gradients of 40 and 75%, and the interface between the layers was collected to retrieve LP cells. Stromal cells were identified as CD45$^-$ Viaprobe$^-$ cells. For fluorescence-activated cell-sorting (FACS) analysis of ILCs, isolated LP cells were further purified by magnetic-activated cell sorting so as to eliminate CD11b$^+$, CD11c$^+$, and CD19$^+$ cells. CD11b$^-$ CD11c$^-$ CD19$^-$ Viaprobe$^-$ CD45$^+$ LP cells were used to detect ILCs.

Antibodies and flow cytometry

For flow cytometric analysis, isolated intestinal ECs were stained with UEA-1-TRITC, anti-CD45–Pacific blue (PB; Biolegend, San Diego, CA), and Viaprobe (BD Biosciences, East Rutherford, NJ). Viaprobe$^-$ CD45$^-$ UEA-1$^+$ cells were identified as F-ECs. After blocking with anti-CD16/32 (FcγRII/III) (BD Biosciences), the following antibodies were used to stain spleen and LP cells: anti-CD45–PB (Biolegend), anti-CD11b–phycoerythrin (PE), anti-Foxp3-fluorescein isothiocyanate (FITC) (eBioscience, San Diego, CA), anti-CD11c–allophycocyanin (APC), anti-CD11b–FITC, anti-Gr-1-Alexa647, anti-CD3-APC, anti-B220-PE, anti-B220-APC, anti-IgA-FITC, anti-CD4-eFluor450, anti-CD90.2–FITC, anti-IL-17-PE, and anti-IFNγ-FITC (all from BD Biosciences), and Viaprobe. CD11b$^-$ CD11c$^-$ CD19$^-$ LP cells were purified by using anti-CD11b, anti-CD11c, and anti-CD19 MicroBeads (Miltenyi Biotec, Bergisch Gladbach, Germany). The results were obtained by using a FACSAria cell sorter (BD Biosciences) with FlowJo software (TreeStar, Ashland, Oregon).

Intracellular staining of Foxp3 and cytokines

Isolated LP cells were incubated for 4 hours at 37°C with 50 ng/mL phorbol myristate acetate (Sigma), 500 ng/mL ionomycin (Sigma), and GolgiPlug (BD Bioscience) in RPMI 1640 containing 10% FCS and penicillin and streptomycin. After incubation, cells were stained with antibodies against surface antigens for 30 min at 4°C. The cells were fixed and permeabilized with Cytofix/Cytoperm solution (BD Bioscience), and cytokines were stained with the fluorescence-conjugated cytokine antibodies. A Foxp3 staining buffer set (eBioscience) was used for intracellular staining of Foxp3.

Depletion of CD90$^+$ ILCs

Depletion of CD90$^+$ ILCs was performed as previously described, with some modifications (*36*). Two hundred and fifty micrograms of a mAb to CD90.2 or an isotype control rat IgG2b (BioXCell, West Lebanon, NH) was given by means of intraperitoneal injection a total of three times at

3-day intervals. Intestinal ECs and LP cells were collected 2 days after the final injection.

Hydrodynamic IL-22 gene delivery system

pLIVE control plasmid (Takara Bio, Shiga, Japan) or IL-22–expressing pLIVE vector (pLIVE-*mIl22*) was introduced into 8-week-old antibiotic-treated C57BL/6 or *Rorc*$^{gfp/gfp}$ mice. Ten micrograms per mouse of plasmid diluted in ~1.5 mL TransIT-EE Hydrodynamic Delivery Solution (Mirus Bio, Madison, WI) was injected via the tail vein within 7 to 10 s. To assess IL-22 expression, serum IL-22 was quantified by means of an enzyme-linked immunosorbent assay (R&D Systems, Minneapolis, MN).

Generation of PP-null mice

mAb to IL-7R (A7R34) was kindly provided by S. Nishikawa. PP-null mice were generated by injecting 600 μg of mAb to IL-7R into pregnant mice on embryonic day 14 (*55*).

In vivo treatment with LTβR-Ig and antibody to IL-22

Neutralization antibody to IL-22 was purchased from eBioscience. Eight-week-old Rag-deficient mice were injected intraperitoneally with antibody to IL-22 a total of five times at 3-day intervals (on days 0, 3, 6, 9, and 12). Plasmid pMKIT-expressing LTβR-Ig and LTβR-Ig treatment was performed as described previously (*56*). Four-week-old C57BL/6 mice were injected intraperitoneally once a week for 3 weeks (on days 0, 7, 14, and 21) with LTβR-Ig fusion protein or control human IgG1 at a dose of 50 μg per mouse. Intestinal ECs were analyzed 3 days after the indicated injection time points.

Adoptive transfer of mixed BM

For mixed BM transfer experiments, *Rorc*$^{gfp/gfp}$ mice were irradiated with two doses of 550 rad each, 3 hours apart. BM cells (1×10^7) from *Rorc*$^{gfp/gfp}$ mice was mixed with BM cells (1×10^7) from C57BL/6 or *Ltα*$^{-/-}$ mice and intravenously injected into irradiated recipient mice. BM chimeric mice were used for experiments 8 weeks after the BM transfer.

Isolation of RNA and real-time reverse transcriptase PCR analysis

Intestinal ECs and subsets of LP cells were sorted with a FACSAria cell sorter (BD Biosciences). The sorted cells were lysed in TRIzol reagent (Invitrogen), and total RNA was extracted in accordance with the manufacturer's instructions. RNA was reverse-transcribed by using a SuperScript VILO cDNA Synthesis Kit (Invitrogen). The cDNA was subjected to real-time reverse transcriptase–PCR (rRT-PCR) by using Roche (Basel, Switzerland) universal probe/primer sets specific for *Ltα* (primer F: 5′-tccctcagaagcacttgacc-3′, R: 5′-gagttctgcttgctggggta-3′, probe No. 62), *Ltβ* (primer F: 5′-cctggtgaccctgttgttg-3′, R: 5′-tgctcctgagccaatgatct-3′, probe No. 76), *Il22* (primer F: 5′-ttcctgaccaaactcagca-3′, R: 5′-tctggatgttctggtcgtca-3′, probe No. 17), *Il22r1* (primer F: 5′;-tgctctgttatctgggctacaa-3′, R: 5′-tcaggacacgttggacgtt-3′, probe No. 9), *Il10rβ* (primer F: 5′-attcggagtgggtcaatgtc-3′, R: 5′-gcatctcaggaggtccaatg-3′, probe No. 29), *Fut2* (primer F: 5′-tgtgacttccaccatcatcc-3′, R: 5′-tctgacagggtttggagctt-3′, probe No. 67), and *Gapdh* (primer F: 5′-tgtccgtcgtggatctgac-3′, R: 5′-cctgcttcaccaccttcttg-3′, probe No. 80). RT-PCR analysis was performed with a Lightcycler II instrument (Roche Diagnostics) to measure the expression levels of specific genes.

Infection with S. typhimurium

Streptomycin-resistant wild-type *S. typhimurium* was isolated from *S. typhimurium* strain ATCC 14028. *Fut2*$^{-/-}$ (BALB/c background) and control littermate mice pretreated with 20 mg of streptomycin 24 hours before infection were given 1×10^8 colony-forming units of the isolated *S. typhimurium* via oral gavage. After 24 hours, the mice were dissected, and the cecal contents were collected. Isolated cecum was treated with PBS containing 0.1 mg mL^{-1} gentamicin at 4°C for 30 min so as to kill bacteria on the tissue surface. The cecum was then homogenized and serial dilutions plated in order to determine the number of *S. typhimurium*. Sections of proximal colon were prepared 48 hours after infection. Infiltration of inflammatory cells was confirmed with hematoxylin and eosin staining.

Statistical analysis

Statistical analysis was performed with an unpaired, two-tailed Student's *t*-test. P values <0.05 were considered statistically significant.

REFERENCES AND NOTES

1. Y. Goto, I. I. Ivanov, Intestinal epithelial cells as mediators of the commensal-host immune crosstalk. *Immunol. Cell Biol.* **91**, 204–214 (2013). doi: 10.1038/icb.2012.80; pmid: 23318659
2. J. Qiu *et al.*, Group 3 innate lymphoid cells inhibit T-cell-mediated intestinal inflammation through aryl hydrocarbon receptor signaling and regulation of microflora. *Immunity* **39**, 386–399 (2013). doi: 10.1016/j.immuni.2013.08.002; pmid: 23954130
3. S. L. Sanos *et al.*, RORgammat and commensal microflora are required for the differentiation of mucosal interleukin 22-producing NKp46$^+$ cells. *Nat. Immunol.* **10**, 83–91 (2009). doi: 10.1038/ni.1684; pmid: 19029903
4. N. Satoh-Takayama *et al.*, Microbial flora drives interleukin 22 production in intestinal NKp46$^+$ cells that provide innate mucosal immune defense. *Immunity* **29**, 958–970 (2008). doi: 10.1016/j.immuni.2008.11.001; pmid: 19084435
5. S. Vaishnava *et al.*, The antibacterial lectin RegIIIγ promotes the spatial segregation of microbiota and host in the intestine. *Science* **334**, 255–258 (2011). doi: 10.1126/science.1209791; pmid: 21998396
6. L. Bry, P. G. Falk, T. Midtvedt, J. I. Gordon, A model of host-microbial interactions in an open mammalian ecosystem. *Science* **273**, 1380–1383 (1996). doi: 10.1126/science.273.5280.1380; pmid: 8703071
7. L. E. Comstock, D. L. Kasper, Bacterial glycans: Key mediators of diverse host immune responses. *Cell* **126**, 847–850 (2006). doi: 10.1016/j.cell.2006.08.021; pmid: 16959564
8. M. J. Coyne, B. Reinap, M. M. Lee, L. E. Comstock, Human symbionts use a host-like pathway for surface fucosylation. *Science* **307**, 1778–1781 (2005). doi: 10.1126/science.1106469; pmid: 15774760
9. L. V. Hooper, J. Xu, P. G. Falk, T. Midtvedt, J. I. Gordon, A molecular sensor that allows a gut commensal to control its nutrient foundation in a competitive ecosystem. *Proc. Natl. Acad. Sci. U.S.A.* **96**, 9833–9838 (1999). doi: 10.1073/pnas.96.17.9833; pmid: 10449780
10. Y. Goto, H. Kiyono, Epithelial barrier: An interface for the cross-communication between gut flora and immune system. *Immunol. Rev.* **245**, 147–163 (2012). doi: 10.1111/j.1600-065X.2011.01078.x; pmid: 22168418
11. K. Terahara *et al.*, Distinct fucosylation of M cells and epithelial cells by Fut1 and Fut2, respectively, in response to intestinal environmental stress. *Biochem. Biophys. Res. Commun.* **404**, 822–828 (2011). doi: 10.1016/j.bbrc.2010.12.067; pmid: 21172308
12. E. A. Hurd, S. E. Domino, Increased susceptibility of secretor factor gene Fut2-null mice to experimental vaginal candidiasis. *Infect. Immun.* **72**, 4279–4281 (2004). doi: 10.1128/IAI.72.7.4279-4281.2004; pmid: 15213174
13. A. Franke *et al.*, Genome-wide meta-analysis increases to 71 the number of confirmed Crohn's disease susceptibility loci. *Nat. Genet.* **42**, 1118–1125 (2010). doi: 10.1038/ng.717; pmid: 21102463
14. A. Hazra *et al.*, Common variants of FUT2 are associated with plasma vitamin B12 levels. *Nat. Genet.* **40**, 1160–1162 (2008). doi: 10.1038/ng.210; pmid: 18776911
15. L. Lindesmith *et al.*, Human susceptibility and resistance to Norwalk virus infection. *Nat. Med.* **9**, 548–553 (2003). doi: 10.1038/nm860; pmid: 12692541
16. D. P. McGovern *et al.*, International IBD Genetics Consortium, Fucosyltransferase 2 (FUT2) non-secretor status is associated with Crohn's disease. *Hum. Mol. Genet.* **19**, 3468–3476 (2010). doi: 10.1093/hmg/ddq248; pmid: 20570966
17. D. J. Smyth *et al.*, FUT2 nonsecretor status links type 1 diabetes susceptibility and resistance to infection. *Diabetes* **60**, 3081–3084 (2011). doi: 10.2337/db11-0638; pmid: 22025780
18. B. M. Imbert-Marcille *et al.*, A FUT2 gene common polymorphism determines resistance to rotavirus A of the P[8] genotype. *J. Infect. Dis.* **209**, 1227–1230 (2014). doi: 10.1093/infdis/jit655; pmid: 24277741
19. T. Folseraas *et al.*, Extended analysis of a genome-wide association study in primary sclerosing cholangitis detects multiple novel risk loci. *J. Hepatol.* **57**, 366–375 (2012). doi: 10.1016/j.jhep.2012.03.031; pmid: 22521342
20. P. C. Kashyap *et al.*, Genetically dictated change in host mucus carbohydrate landscape exerts a diet-dependent effect on the gut microbiota. *Proc. Natl. Acad. Sci. U.S.A.* **110**, 17059–17064 (2013). doi: 10.1073/pnas.1306070110; pmid: 24062455
21. P. Rausch *et al.*, Colonic mucosa-associated microbiota is influenced by an interaction of Crohn disease and FUT2 (Secretor) genotype. *Proc. Natl. Acad. Sci. U.S.A.* **108**, 19030–19035 (2011). doi: 10.1073/pnas.1106408108; pmid: 22068912
22. R. B. Sartor, Microbial influences in inflammatory bowel diseases. *Gastroenterology* **134**, 577–594 (2008). doi: 10.1053/j.gastro.2007.11.059; pmid: 18242222
23. J. P. Koopman, A. M. Stadhouders, H. M. Kennis, H. De Boer, The attachment of filamentous segmented micro-organisms to the distal ileum wall of the mouse: A scanning and transmission electron microscopy study. *Lab. Anim.* **21**, 48–52 (1987). doi: 10.1258/002367787780740743; pmid: 3560864
24. K. Suzuki *et al.*, Aberrant expansion of segmented filamentous bacteria in IgA-deficient gut. *Proc. Natl. Acad. Sci. U.S.A.* **101**, 1981–1986 (2004). doi: 10.1073/pnas.0307317101; pmid: 14766966
25. V. Gaboriau-Routhiau *et al.*, The key role of segmented filamentous bacteria in the coordinated maturation of gut helper T cell responses. *Immunity* **31**, 677–689 (2009). doi: 10.1016/j.immuni.2009.08.020; pmid: 19833089
26. I. I. Ivanov *et al.*, Induction of intestinal Th17 cells by segmented filamentous bacteria. *Cell* **139**, 485–498 (2009). doi: 10.1016/j.cell.2009.09.033; pmid: 19836068
27. I. I. Ivanov *et al.*, Specific microbiota direct the differentiation of IL-17-producing T-helper cells in the mucosa of the small intestine. *Cell Host Microbe* **4**, 337–349 (2008). doi: 10.1016/j.chom.2008.09.009; pmid: 18854238
28. C. P. Davis, D. C. Savage, Habitat, succession, attachment, and morphology of segmented, filamentous microbes indigenous to the murine gastrointestinal tract. *Infect. Immun.* **10**, 948–956 (1974). pmid: 4426712
29. Y. Umesaki, H. Setoyama, S. Matsumoto, A. Imaoka, K. Itoh, Differential roles of segmented filamentous bacteria and clostridia in development of the intestinal immune system. *Infect. Immun.* **67**, 3504–3511 (1999).pmid: 10377132
30. I. I. Ivanov *et al.*, The orphan nuclear receptor RORγt directs the differentiation program of proinflammatory IL-17$^+$ T helper cells. *Cell* **126**, 1121–1133 (2006). doi: 10.1016/j.cell.2006.07.035; pmid: 16990136
31. H. Spits *et al.*, Innate lymphoid cells—A proposal for uniform nomenclature. *Nat. Rev. Immunol.* **13**, 145–149 (2013). doi: 10.1038/nri3365; pmid: 23348417
32. H. Spits, J. P. Di Santo, The expanding family of innate lymphoid cells: Regulators and effectors of immunity and tissue remodeling. *Nat. Immunol.* **12**, 21–27 (2011). doi: 10.1038/ni.1962; pmid: 21113163

33. Y. Yokota *et al.*, Development of peripheral lymphoid organs and natural killer cells depends on the helix-loop-helix inhibitor Id2. *Nature* **397**, 702–706 (1999). doi: 10.1038/17812; pmid: 10067894
34. G. Eberl *et al.*, An essential function for the nuclear receptor RORγ(t) in the generation of fetal lymphoid tissue inducer cells. *Nat. Immunol.* **5**, 64–73 (2004). doi: 10.1038/ni1022; pmid: 14691482
35. S. Sawa *et al.*, RORγt$^+$ innate lymphoid cells regulate intestinal homeostasis by integrating negative signals from the symbiotic microbiota. *Nat. Immunol.* **12**, 320–326 (2011). doi: 10.1038/ni.2002; pmid: 21336274
36. G. F. Sonnenberg, L. A. Monticelli, M. M. Elloso, L. A. Fouser, D. Artis, CD4(+) lymphoid tissue-inducer cells promote innate immunity in the gut. *Immunity* **34**, 122–134 (2011). doi: 10.1016/j.immuni.2010.12.009; pmid: 21194981
37. S. Buonocore *et al.*, Innate lymphoid cells drive interleukin-23-dependent innate intestinal pathology. *Nature* **464**, 1371–1375 (2010). doi: 10.1038/nature08949; pmid: 20393462
38. G. Pickert *et al.*, STAT3 links IL-22 signaling in intestinal epithelial cells to mucosal wound healing. *J. Exp. Med.* **206**, 1465–1472 (2009). doi: 10.1084/jem.20082683; pmid: 19564350
39. G. F. Sonnenberg, L. A. Fouser, D. Artis, Functional biology of the IL-22-IL-22R pathway in regulating immunity and inflammation at barrier surfaces. *Adv. Immunol.* **107**, 1–29 (2010). doi: 10.1016/B978-0-12-381300-8.00001-0; pmid: 21034969
40. M. Tsuji *et al.*, Requirement for lymphoid tissue-inducer cells in isolated follicle formation and T cell-independent immunoglobulin A generation in the gut. *Immunity* **29**, 261–271 (2008). doi: 10.1016/j.immuni.2008.05.014; pmid: 18656387
41. P. De Togni *et al.*, Abnormal development of peripheral lymphoid organs in mice deficient in lymphotoxin. *Science* **264**, 703–707 (1994). doi: 10.1126/science.8171322; pmid: 8171322
42. D. Chessa, M. G. Winter, M. Jakomin, A. J. Bäumler, *Salmonella enterica* serotype Typhimurium Std fimbriae bind terminal α (1,2)fucose residues in the cecal mucosa. *Mol. Microbiol.* **71**, 864–875 (2009). doi: 10.1111/j.1365-2958.2008.06566.x; pmid: 19183274
43. M. Awoniyi, S. I. Miller, C. B. Wilson, A. M. Hajjar, K. D. Smith, Homeostatic regulation of *Salmonella*-induced mucosal inflammation and injury by IL-23. *PLOS One* **7**, e37311 (2012). doi: 10.1371/journal.pone.0037311; pmid: 22624013
44. I. Godinez *et al.*, T cells help to amplify inflammatory responses induced by *Salmonella enterica* serotype Typhimurium in the intestinal mucosa. *Infect. Immun.* **76**, 2008–2017 (2008). doi: 10.1128/IAI.01691-07; pmid: 18347048
45. A. V. Tumanov *et al.*, Lymphotoxin controls the IL-22 protection pathway in gut innate lymphoid cells during mucosal pathogen challenge. *Cell Host Microbe* **10**, 44–53 (2011). doi: 10.1016/j.chom.2011.06.002; pmid: 21767811
46. S. E. Domino, L. Zhang, P. J. Gillespie, T. L. Saunders, J. B. Lowe, Deficiency of reproductive tract α(1,2)fucosylated glycans and normal fertility in mice with targeted deletions of the FUT1 or FUT2 α(1,2)fucosyltransferase locus. *Mol. Cell. Biol.* **21**, 8336–8345 (2001). doi: 10.1128/MCB.21.24.8336-8345.2001; pmid: 11713270
47. K. Kreymborg *et al.*, IL-22 is expressed by Th17 cells in an IL-23-dependent fashion, but not required for the development of autoimmune encephalomyelitis. *J. Immunol.* **179**, 8098–8104 (2007). doi: 10.4049/jimmunol.179.12.8098; pmid: 18056351
48. S. Rakoff-Nahoum, J. Paglino, F. Eslami-Varzaneh, S. Edberg, R. Medzhitov, Recognition of commensal microflora by toll-like receptors is required for intestinal homeostasis. *Cell* **118**, 229–241 (2004). doi: 10.1016/j.cell.2004.07.002; pmid: 15260992
49. T. Matsuki *et al.*, Quantitative PCR with 16S rRNA-gene-targeted species-specific primers for analysis of human intestinal bifidobacteria. *Appl. Environ. Microbiol.* **70**, 167–173 (2004). doi: 10.1128/AEM.70.1.167-173.2004; pmid: 14711639
50. R. Kibe, M. Sakamoto, H. Hayashi, H. Yokota, Y. Benno, Maturation of the murine cecal microbiota as revealed by terminal restriction fragment length polymorphism and 16S rRNA gene clone libraries. *FEMS Microbiol. Lett.* **235**, 139–146 (2004). doi: 10.1111/j.1574-6968.2004.tb09578.x; pmid: 15158273
51. M. H. Jang *et al.*, Intestinal villous M cells: An antigen entry site in the mucosal epithelium. *Proc. Natl. Acad. Sci. U.S.A.* **101**, 6110–6115 (2004). doi: 10.1073/pnas.0400969101; pmid: 15071180
52. T. Obata *et al.*, Indigenous opportunistic bacteria inhabit mammalian gut-associated lymphoid tissues and share a mucosal antibody-mediated symbiosis. *Proc. Natl. Acad. Sci. U.S.A.* **107**, 7419–7424 (2010). doi: 10.1073/pnas.1001061107; pmid: 20360558
53. M. Yamamoto, K. Fujihashi, K. Kawabata, J. R. McGhee, H. Kiyono, A mucosal intranet: Intestinal epithelial cells down-regulate intraepithelial, but not peripheral, T lymphocytes. *J. Immunol.* **160**, 2188–2196 (1998). ; pmid: 9498757
54. N. Ohta *et al.*, IL-15-dependent activation-induced cell death-resistant Th1 type CD8 α β$^+$NK1.1$^+$ T cells for the development of small intestinal inflammation. *J. Immunol.* **169**, 460–468 (2002). doi: 10.4049/jimmunol.169.1.460; pmid: 12077277
55. H. Yoshida *et al.*, IL-7 receptor α$^+$ CD3(-) cells in the embryonic intestine induces the organizing center of Peyer's patches. *Int. Immunol.* **11**, 643–655 (1999). doi: 10.1093/intimm/11.5.643; pmid: 10330270
56. M. Yamamoto *et al.*, Role of gut-associated lymphoreticular tissues in antigen-specific intestinal IgA immunity. *J. Immunol.* **173**, 762–769 (2004). doi: 10.4049/jimmunol.173.2.762; pmid: 15240662

ACKNOWLEDGMENTS

We thank M. Shimaoka, G. Eberl, M. Pasparakis, K. Honda, C. A. Hunter, C. O. Elson, and J. R. Mora for their critical and helpful comments and advice on this research. Y. Yokota and M. Yamamoto kindly provided Id2-deficient mice and LTβR-Ig, respectively. R. Curtis III and H. Matsui kindly provided several strains of *Salmonella typhimurium*. We thank Y. Akiyama for her technical support with the *S. typhimurium* infection model. S. Tanaka gave us helpful technical suggestions for performing flow cytometric analysis. The data presented in this paper are tabulated in the main paper and in the supplementary materials. Sequences of the bacterial 16S rRNA genes obtained from duodenal and ileal mucus bacteria have been deposited in the International Nucleotide Sequence Database (accession nos. AB470733 to AB470815). This work was supported by grants from the following sources: the Core Research for Evolutional Science and Technology Program of the Japan Science and Technology Agency (to H.K.); a Grant-in-Aid for Scientific Research on Priority Areas, Scientific Research (S) (to H.K.); Specially Promoted Research (230000-12 to C.S.); Scientific Research (B) (to J.K.); for the Leading-edge Research Infrastructure Program and the Young Researcher Overseas Visits Program for Vitalizing Brain Circulation (to Y.G., J.K., and H.K.); for the Leading-edge Research Infrastructure Program (to J.K. and H.K.) from the Ministry of Education, Culture, Sports, Science and Technology of Japan; the Global Center of Excellence (COE) Program "Center of Education and Research for Advanced Genome-based Medicine" (to H.K.); the Ministry of Health, Labor and Welfare of Japan (to J.K. and H.K.); the Science and Technology Research Promotion Program for Agriculture, Forestry, Fisheries and Food Industry (to J.K.); Mochida Memorial Foundation for Medical and Pharmaceutical Research (to J.K.); the National Institutes of Health (1R01DK098378 to I.I.); and by the Crohn's and Colitis Foundation of America (SRA#259540 to I.I.). The authors declare no conflicts of interest.

SUPPLEMENTARY MATERIALS

www.sciencemag.org/content/345/6202/1254009/suppl/DC1
Figs. S1 to S11
Table S1

27 March 2014; accepted 25 July 2014
10.1126/science.1254009

Regulation of Intestinal IgA Responses by Dietary Palmitic Acid and Its Metabolism

Jun Kunisawa,[*,†,‡,§,¶] Eri Hashimoto,[*,†] Asuka Inoue,[‡,‖] Risa Nagasawa,[*,†] Yuji Suzuki,[†] Izumi Ishikawa,[†] Shiori Shikata,[*,†] Makoto Arita,[#,**,1] Junken Aoki,[††,‖] and Hiroshi Kiyono[†,‡,††,‡‡,§§]

Enhancement of intestinal IgA responses is a primary strategy in the development of oral vaccine. Dietary fatty acids are known to regulate host immune responses. In this study, we show that dietary palmitic acid (PA) and its metabolites enhance intestinal IgA responses. Intestinal IgA production was increased in mice maintained on a PA-enriched diet. These mice also showed increased intestinal IgA responses against orally immunized Ag, without any effect on serum Ab responses. We found that PA directly stimulates plasma cells to produce Ab. In addition, mice receiving a PA-enriched diet had increased numbers of IgA-producing plasma cells in the large intestine; this effect was abolished when serine palmitoyltransferase was inhibited. These findings suggest that dietary PA regulates intestinal IgA responses and has the potential to be a diet-derived mucosal adjuvant. ***The Journal of Immunology*****, 2014, 193: 000–000.**

High levels of IgA are present in the intestine, where they protect the host against pathogenic microorganisms by preventing their attachment to and entrance into epithelial cells, as well as by neutralizing their toxins (1). Some patients with IgA deficiency show increased susceptibility to infectious pathogens, including *Giardia lamblia*, *Campylobacter*, *Clostridium*, *Salmonella*, and rotavirus (2). Given the immunologic importance of IgA in immunosurveillance in the intestine, the primary goal of effective oral vaccines is the efficient induction of Ag-specific IgA responses (3).

An efficient intestinal IgA response requires host-derived factors, including cytokines (e.g., IL-5, IL-6, IL-10, IL-15, APRIL, BAFF) and chemokines (e.g., CCL25/CCR9) (4, 5), as well as immunologic cross-talk with environmental factors (e.g., commensal bacteria and dietary materials) (6). Indeed, germ-free mice have decreased intestinal IgA responses because of the immature structure of Peyer's patches (PPs) and isolated lymphoid follicles (7, 8). We recently identified a unique subset of intestinal IgA-producing plasma cells (PCs) in the murine intestine; these cells expressed CD11b, required microbial stimulation and mature PP structure, proliferated vigorously, and produced high amounts of IgA (9).

In addition to commensal bacteria, nutritional molecules, such as vitamins, are essential for the development, maintenance, and regulation of intestinal immune responses (6, 10, 11). Therefore, nutritional deficiencies and inappropriate dietary intake increase the risk for infectious, allergic, and inflammatory diseases (12, 13). Among various dietary factors, oils are known to influence host immune function and inflammatory responses (14–16). Overnutrition due to a high-fat diet leads to the development of inflammation in adipose tissue, which is frequently associated with obesity and atherosclerosis (17). Recent findings suggest that, in addition to the quantity of oil ingested, the fatty acid (FA) composition of the oil is an important factor in various immunologic and inflammatory conditions (14–16). Dietary oil is generally composed of long-chain saturated FAs (e.g., C16:0 palmitic acid [PA] and C18:0 stearic acid) and mono- or polyunsaturated FAs (PUFAs; e.g., C18:1 oleic acid, C18:2 linoleic acid, and C18:3 α-linolenic acid). α-Linolenic acid and linoleic acid are precursors of ω3 and ω6 PUFAs, respectively; ω3 FAs are metabolized into anti-inflammatory molecules, whereas ω6 FAs are converted into proinflammatory lipid mediators (16, 18). Therefore, the ratio of α-linolenic acid/linoleic acid in dietary oils is thought to determine the onset of various immunologic conditions. In addition to modulating the ω3–ω6 PUFA balance, saturated FAs, such as PA, stimulate host immune responses by promoting the production of proinflammatory cytokines, including IL-6 and TNF-α (19, 20). Although these proinflammatory cytokines are prerequisite factors for the efficient induction of IgA

*Laboratory of Vaccine Materials, National Institute of Biomedical Innovation, Osaka 567-0085, Japan; †Division of Mucosal Immunology, Department of Microbiology and Immunology, The Institute of Medical Science, University of Tokyo, Tokyo 108-8639, Japan; ‡International Research and Development Center for Mucosal Vaccines, The Institute of Medical Science, University of Tokyo, Tokyo 108-8639, Japan; §Department of Microbiology and Immunology, Kobe University School of Medicine, Kobe 650-0017, Japan; ¶Graduate School of Pharmaceutical Sciences and Graduate School of Dentistry, Osaka University, Osaka 565-0871, Japan; ‖Laboratory of Molecular and Cellular Biochemistry, Graduate School of Pharmaceutical Sciences, Tohoku University, Sendai 980-8578, Japan; #Department of Health Chemistry, Graduate School of Pharmaceutical Sciences, University of Tokyo, Tokyo 113-0033, Japan; **Precursory Research for Embryonic Science and Technology, Japan Science and Technology Agency, Saitama 332-0012, Japan; ††Core Research for Evolutional Science and Technology, Japan Science and Technology Agency, Saitama 332-0012, Japan; ‡‡Department of Medical Genome Science, Graduate School of Frontier Science, University of Tokyo, Chiba 277-8561, Japan; and §§Graduate School of Medicine, University of Tokyo, Tokyo 113-0033, Japan

[1]Current address: Laboratory for Metabolomics, RIKEN Center for Integrative Medical Sciences, Yokohama, Kanagawa, Japan.

Received for publication November 1, 2013. Accepted for publication June 11, 2014.

This work was supported by grants from the Science and Technology Research Promotion Program for Agriculture, Forestry, Fisheries, and Food Industry (to J.K.); the Program for Promotion of Basic and Applied Research for Innovations in Bio-oriented Industry (to J.K.); the Ministry of Education, Culture, Sports, Science, and Technology of Japan (to J.K., M.A., J.A., and H.K.); the Ministry of Health and Welfare of Japan (to J.K. and H.K.); the Yakult Bio-Science Foundation (to J.K.); the Ono Medical Research Foundation (to J.K.); the Japan Science and Technology Agency, Core Research for Evolutional Science and Technology (to J.A. and H.K.); and Precursory Research for Embryonic Science and Technology (to M.A.).

Address correspondence and reprint requests to Dr. Jun Kunisawa, Laboratory of Vaccine Materials, National Institute of Biomedical Innovation, 7-9-8 Asagi Saito, Osaka 567-0085, Japan. E-mail address: kunisawa@nibio.go.jp

The online version of this article contains supplemental material.

Abbreviations used in this article: CT, cholera toxin; FA, fatty acid; iLP, intestinal lamina propria; PA, palmitic acid; PC, plasma cell; PP, Peyer's patch; PUFA, polyunsaturated fatty acid; S1P, sphingosine 1 phosphate; SPT, serine palmitoyltransferase.

www.jimmunol.org/cgi/doi/10.4049/jimmunol.1302944

responses (5), the immunologic function of dietary PA in the control of IgA production remained to be investigated. In this study, we show that PA-enriched diets enhance intestinal IgA responses both directly and through their metabolic pathways.

Materials and Methods

Mice

Female BALB/c, C3H/HeJ, and C3H/HeN mice were purchased from CLEA Japan (Tokyo, Japan). Chemically defined AIN-93M–based diets containing soybean, palm, or coconut oil or soybean oil plus supplemental purified PA were from Oriental Yeast (Tokyo, Japan). All mice were provided with a sterile diet and water ad libitum. To inhibit serine palmitoyltransferase (SPT) activity, mice were treated with myriocin (1.0 mg/kg i.p. daily; Sigma-Aldrich, St. Louis, MO) for 4 d (21). All mice were maintained in the experimental animal facility at the University of Tokyo and National Institute of Biomedical Innovation; the experiments were approved by the Animal Care and Use Committee of each institute and conducted in accordance with their guidelines.

Cell isolation

To isolate mononuclear cells from PPs, we stirred intestinal tissues in RPMI 1640 medium containing 2% FCS and 0.5 mg/ml collagenase (Wako, Osaka, Japan). Cells were isolated from the intestinal lamina propria (iLP) as previously described (9, 22). Briefly, PPs were removed, and small and large intestines were cut into 2-cm pieces, which were stirred in RPMI 1640 containing 1 mM EDTA and 2% FCS. Then the tissues were stirred in collagenase for 15 min three times (small intestine, 0.8 mg/ml; large intestine, 1.6 mg/ml) before undergoing discontinuous Percoll gradient centrifugation. Lymphocytes were isolated at the interface between the 40 and 75% layers.

Oral immunization

Mice received sodium bicarbonate to neutralize gastric acid before oral immunization (9, 22). Thirty minutes later, the mice were immunized orally concurrently with 1 mg OVA (Sigma-Aldrich) and 10 μg cholera toxin (CT; List Biological Laboratories, Campbell, CA). This oral-immunization procedure was conducted on days 0, 7, and 14.

Detection of total Ig by ELISA and OVA-specific Ab responses by ELISPOT assay

Total Ig levels in serum and fecal extracts were determined by ELISA, as previously described (9, 22). To measure Ab concentration, purified murine isotype-specific Abs (BD Biosciences, San Jose, CA) were used as standards for quantification. For the detection of OVA-specific Abs and Ab-forming cells, fecal extracts and iLP were prepared 7 d after the final immunization. Standard OVA-specific ELISAs and ELISPOT assays were performed as previously described (9, 22).

Flow cytometry and cell sorting

Flow cytometry and cell sorting were performed as previously described (9, 22). Cells were preincubated with anti-CD16/32 Ab and then stained with fluorescent Abs specific for B220, IgG1, IgA (all from BD Biosciences), CD19, and CD138 (BioLegend, San Diego, CA). Forward scatter–height and forward scatter–area discrimination was used to exclude doublet cells, and Via-Probe Cell Viability Solution (BD Biosciences) was used to discriminate between dead and living cells. For the BrdU-uptake assay, mice received 1 mg BrdU i.p., and the BrdU signal was detected according to the manufacturer's protocol (BD Biosciences) (9). Concentration-matched isotype Abs were used as negative controls. Flow cytometric analysis and cell sorting were carried out using FACSCanto II and FACSAria (BD Biosciences), respectively. We confirmed that cell purity was ~95%.

In vitro culture of PCs with PA

Stock solutions containing 5 mM PA and 10% BSA were prepared as previously reported (23). Purified IgA^+ $B220^-$ PCs isolated from the iLP (10^4 cells/well) or $CD19^+$ $CD138^+$ PCs isolated from the spleen (10^5 cells/well) were cultured with 10 or 100 μM PA for 96 h. The amount of IgA (for iLP) or IgG (for spleen) in the culture supernatant was determined by ELISA, as described earlier.

Measurement of PA in the serum and intestinal tissues

Lipids were extracted from serum and intestinal tissues by using chloroform–methanol and chloroform solutions. The specimens were dried in nitrogen gas and dissolved in 0.4 M potassium methoxide in methanol and 14% boron trifluoride in methanol. The FA concentrations in the solutions were measured (SRL, Tokyo, Japan) using gas chromatography (model GF 17A; Shimazu, Kyoto, Japan).

Statistics

Experimental groups were compared using the Mann–Whitney *U* test (GraphPad, San Diego, CA).

Results

Mice maintained on a diet containing palm oil show enhanced intestinal IgA production

To examine whether dietary PA affects intestinal IgA production, we maintained mice on a diet containing 4% soybean (control) or palm (PA-rich) oil for 2 mo (Fig. 1A) and measured the amounts of fecal IgA. Intestinal IgA production was higher in the mice that received palm oil than in those given soybean oil (Fig. 1B). In contrast, the amounts of serum IgG and IgA were similar between the soybean and palm oil groups (Fig. 1B, Supplemental Fig. 1). Palm oil is high in both PA and oleic acid (Fig. 1A), but mice maintained on a diet containing rapeseed oil, which contained a similar amount of oleic acid as that present in the palm oil, showed no enhancement of intestinal IgA production (data not shown).

We then considered whether other saturated FAs enhance intestinal IgA production. To this end, we used coconut oil, which (like palm oil) is a Palmae plant–based oil but contains large

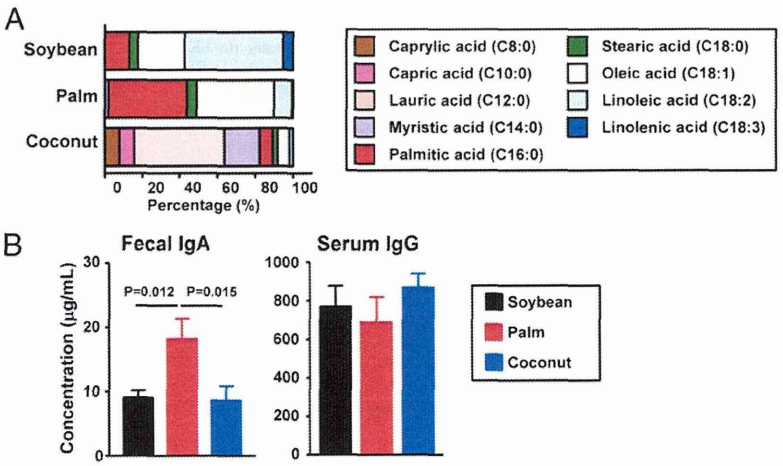

FIGURE 1. Palm oil enhances intestinal IgA production. (**A**) FA composition of soybean, palm, and coconut oils. (**B**) Mice were maintained on a diet containing soybean, palm, or coconut oil for 2 mo. Feces and serum samples were collected for measurement of the amounts of IgA and IgG, respectively (mean ± 1 SD, n = 10/group).